DESIGN, FABRICATION AND CHARACTERIZATION OF A SUSPENDED PLATE MECHANO-OPTICAL MODULATOR

M. B. Syed Nawazuddin[1], M. de Boer[1], J. W. Berenschot[1], K. C. Ma[1], M. Elwenspoek[1,2] and R. J. Wiegerink[1]

[1]MESA+ Institute for Nanotechnology, University of Twente, The Netherlands
and [2]FRIAS, University of Freiburg, Germany

ABSTRACT

A mechano-optical modulator is presented based on the Integrated Optical Nano-Mechanical (IONM) effect [1]. It consists of a light-weight, rigid silicon-nitride suspended plate structure with strengthening ridges and bi-directional electrostatic actuation to maximize switching speed. The mechanical structure and optical waveguide are realized on separate chips and then assembled together resulting in hybrid integration. The latter is made possible by using a self-alignment technique which results in a misalignment error of at most 2 μm.

INTRODUCTION

Mechano-optical modulators based on the IONM effect have been receiving a lot of attention where microsecond response times are sufficiently fast. The main attractive features of such a mechano-optical modulator are the relatively easy fabrication process and relatively high switching speeds in the order of microseconds without the need for electro-optic materials and without the large power consumption of thermo-optic modulators. Both phase and intensity modulation has been reported [2, 3] and several devices based on the IONM effect have been presented [4, 5]. In all these devices, an optically transparent or absorptive material (metal) is moved in and out of the evanescent field, resulting in modulation of the real or imaginary part of the refractive index.

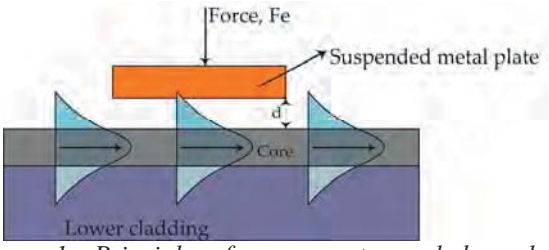

Figure 1: Principle of evanescent coupled mechano-optical modulator

The basic principle of the IONM effect is shown in Figure 1. The air gap d, between the mechanical element and the optical waveguide is varied by an applied electrostatic force. When the air gap is considerably less than the wavelength λ, ($d \leq \lambda$), the evanescent part of the guided wave penetrates through the gap into the mechanical element, giving a change in effective refractive index (N) of the guided mode. A small change in the air gap Δd, can introduce significant changes in the effective refractive index.

Prime focus of the research presented in this paper is the realization of light-weight mechanical structures that can be combined with an optical waveguide to form a fast ON/OFF intensity modulator. The mechanical structure and optical waveguide are realized on separate chips and assembled using a self-alignment technique so that no adjustments are needed in the fabrication process of the waveguide except for some post-processing steps to remove the top cladding and deposit actuation electrodes. In this paper, the design, fabrication and assembly procedure of the suspended plate mechano-optical modulator and its first characterization results are presented.

DESIGN

Figure 2 shows schematic drawings of the mechanical and optical chips assembled on top of each other.

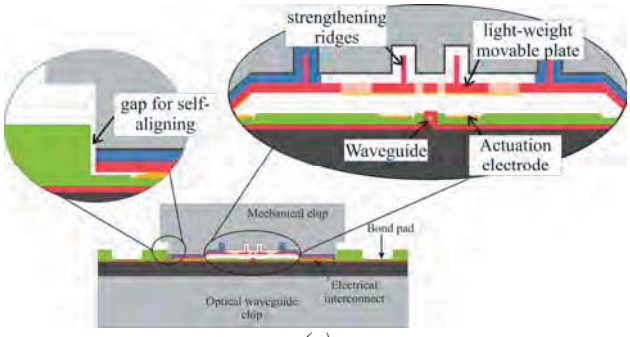

(a)

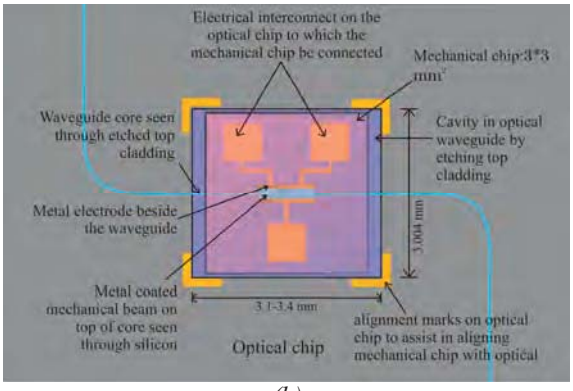

(b)

Figure 2: Schematic representation of integrated device: (a) Cross sectional view of the integrated mechanical chip with the optical waveguide chip and (b) top view.

Optical waveguide design

A multi-layer optical waveguide (MLW) technology called TriPleX is used, which was developed by LioniX BV [6, 7]. Infra-red light with a wavelength of λ=1550 nm and TE polarization is used for the propagating mode. The waveguide is comprised of a composite core which is made of a thin high-index Si_3N_4 layer encapsulating a low-index SiO_2 inner material. Two distinct cross-sectional geometries are possible with this technology: box shape

and A-shape. With both cross sections, the losses due to birefringence, polarization and bending are significantly reduced when compared to conventional and high-index contrast waveguides [6, 7]. Figure 3 shows a cross-sectional drawing of the A-shape TriPleX waveguide used in this study.

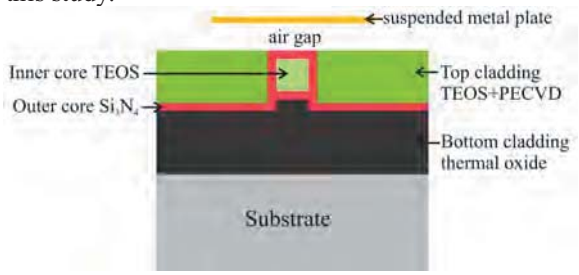

Figure 3: Cross-sectional drawing of A-shape TripleX waveguide

Mechanical suspended plate design

The suspended mechanical element is designed as a free-free beam anchored to the substrate through thin springs. Figure 4 shows schematic drawings of the structure. To allow for fast bi-directional switching, 1 µm thin light-weight suspended plate structures were designed; 35 µm wide and 65 to 125 µm in length, with strengthening ridges underneath.

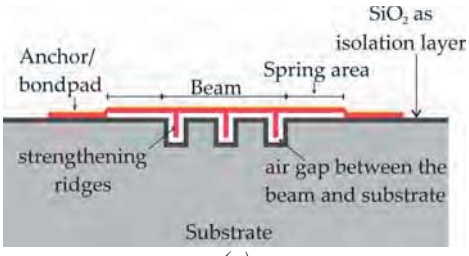

(a)

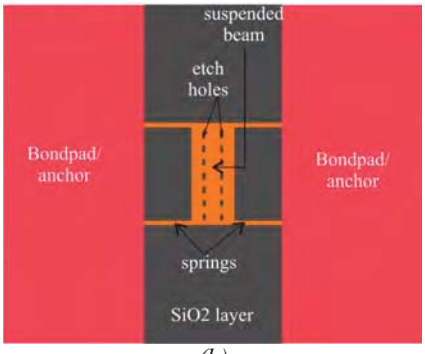

(b)

Figure 4: Schematic drawings of suspended mechanical beam (a) Cross section, (b) Top view

The structure can be modeled as a 2nd order mass-spring-damper system. The mechanical resonance frequency is given by:

$$f = \frac{1}{2\pi}\sqrt{\frac{K}{m + 0.33m_s}} \qquad (1)$$

With K the effective spring constant of the suspension, m the mass of the suspended plate, and m_s is the mass of springs.

In case of electrostatic actuation, pull-in will occur when distance between the electrodes has reduced to 2/3 of the original gap x_0. The pull-in voltage is given by:

$$V_p = \sqrt{\frac{4Kx_0^3}{27\varepsilon_0 A}} \qquad (2)$$

For a beam having dimension l = 125 µm, w = 35 µm and t = 1µm, the calculated mass, spring constant, resonance frequency and static pull-in voltage are given in Table 1.

Table 1: Calculated values of mechanical beam parameters

Parameter	Value
Mass-beam (10^{-12} kg)	15.7
Mass-spring (10^{-12} kg)	3.8
Spring constant (N/m)	20.1
Resonance frequency (kHz)	173.7
Static pull-in voltage (V)	22.8

For the first batch of devices, gold (Au) electrodes were deposited on top of the structures, both for actuation and for modulation of the evanescent field. Bi-directional actuation is achieved by using both the silicon bulk of the mechanical chip and electrodes deposited next to the waveguide (see Figure 2 & 6) as counter-electrodes.

Concept validation

Field Designer, a mode solver tool developed by PhoeniX BV [8], was used for conceptual validation of the integrated mechano-optical modulator. It uses film mode matching and finite difference methods to extract the mode fields.

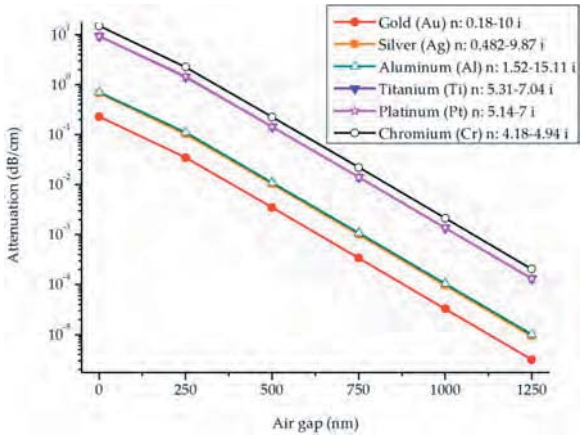

Figure 5: Graph showing loss due to different metals with varying air gap width

The main design parameter here is the required air gap distance between the optical waveguide and the mechanical chip to have loss free propagation of optical signal in its ON state. Mode field analyses were done for various metals as a function of the distance between the metal layer and the optical waveguide. Figure 5 shows the calculated loss. It is clear that gold is not the optimal choice to introduce absorption loss and much better results can be expected from chromium, platinum or titanium.

FABRICATION

The TriPleX waveguide is fabricated following the process developed by LioniX as described in [6, 7]. The processing is performed on silicon substrates containing 8 µm thick thermal oxide, which acts as the lower cladding

of waveguide. The fabrication process starts with the deposition of a thin Si_3N_4 layer, which forms the bottom side of the high-index outer core, and is followed by the deposition of TEOS oxide, the low-index inner core. Next, the TEOS oxide is patterned by reactive ion etching (RIE) and the top Si_3N_4 layer is deposited. The pattern in the TEOS layer is also used to realize anti-stiction bumps, to prevent stiction of the suspended plate to the waveguide chip. The waveguide fabrication process is completed with the deposition of a thick TEOS layer and a very thick layer of PECVD (4 µm) oxides to form the top cladding. Finally, post-processing steps are performed to locally remove the top cladding layer and deposit the gold actuation electrodes. Figure 6 shows a photograph of the realized waveguide with actuation electrodes.

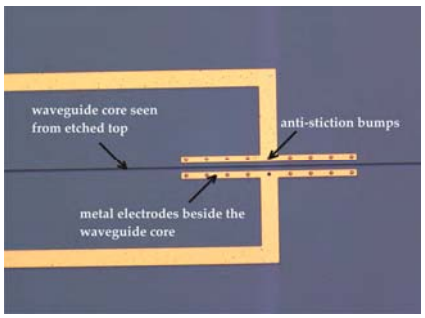

Figure 6: Microscopic image showing the top view of the optical waveguide with actuation electrodes.

The mechanical elements are fabricated using highly conductive silicon substrates. The process starts with the realization of shallow cavities that define the initial distance between the suspended plate and the waveguide after bonding. These cavities are created by local oxidation of silicon followed by removal of oxide.

Figure 7 shows an outline of the fabrication sequence that follows after creating the shallow cavities. The process continues with etching trenches, 5 µm wide and 5 µm deep, to form the strengthening ridges (step 1). Next, the wafer is oxidized (step 2) to get a 1 µm thick oxide layer that will later act as etch stop during sacrificial layer etching. Next, a 1.5 µm thick layer of polysilicon is deposited through LPCVD (step 3), which will be the sacrificial layer that defines the air gap between the released beam and the substrate. Subsequently, a 1 µm thick layer of low-stress silicon-rich silicon nitride (SiRN) is deposited using LPCVD (step 4), which will form the suspended structure. Next, the electrode layer (10 nm Cr + 100 nm Au) is deposited and patterned (steps 5 and 6).

To facilitate self-aligned assembly onto the waveguide chip, the next steps (7 and 8) create a well-defined area of 3×3 mm^2. With photoresist as mask, the stack of SiRN, polysilicon, SiO_2 and the silicon substrate are etched using deep reactive ion etching (DRIE). Next, a thick layer of resist is spun to protect the etched trenches, followed by covering the whole wafer with dicing foil (step 9) to protect the devices during dicing into chips (step 10).

After dicing, the foil is removed keeping the resist on the trenches for protection. Next, the beam with spring structures is released by etching the polysilicon sacrificial layer using XeF_2. Finally, the photoresist is removed in O_2 plasma. Figure 8 shows a photograph of a typical device.

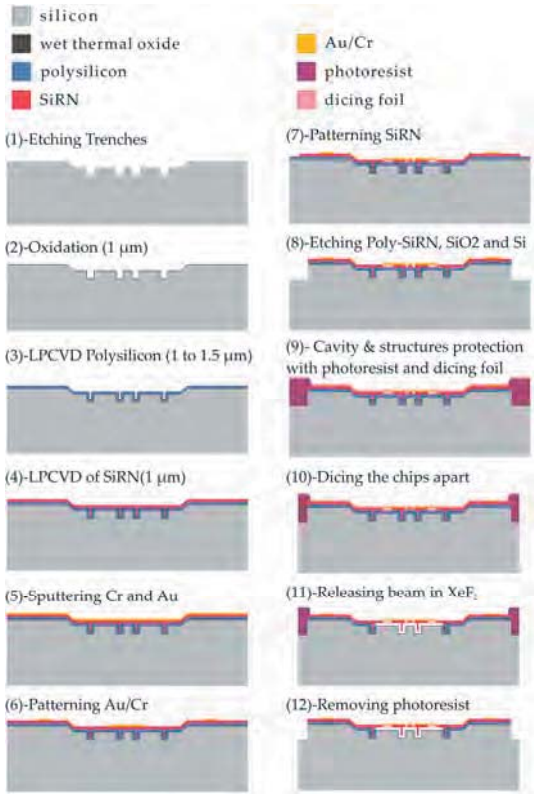

Figure 7: Outline of fabrication steps to realize the mechanical chip to integrated with the optical chip

Self-aligned assembly

Prior to assembly, both chips are cleaned in isopropyl alcohol, which ensures that the surfaces are free of dust particles. The suspended plate structure is self-aligned to the waveguide using etched trenches that exactly coincide with the etched cavity in the top cladding of the waveguide. Once clamped, the suspended plate structure is separated from the waveguide by a well-controlled gap of 1 µm. The lateral alignment accuracy in the direction perpendicular to the waveguide is better than 2 µm. In the longitudinal direction of the waveguide the alignment is not critical and a tolerance of 100 µm was chosen for ease of assembly.

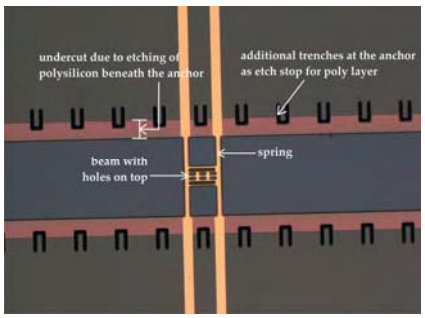

Figure 8: Microscopic image showing the top view of the suspended plate structure

CHARACTERIZATION

The mechanical structures were characterized separately to estimate the pull-in voltage and resonance frequency and the optical waveguides were tested by an insertion loss measurement. The static pull-in measurement is performed by applying a DC voltage

between the gold coated SiRN beam and the substrate. The displacement of the mechanical beam towards the substrate is measured using a White Light Interferometer (WLI). The result of the pull-in measurement for a 125 µm long beam is shown in Figure 9. For the same beam, the resonance frequency was measured using a vibrometer and was found to be 175.6 kHz. These results correspond very well with the calculated values shown in Table 1.

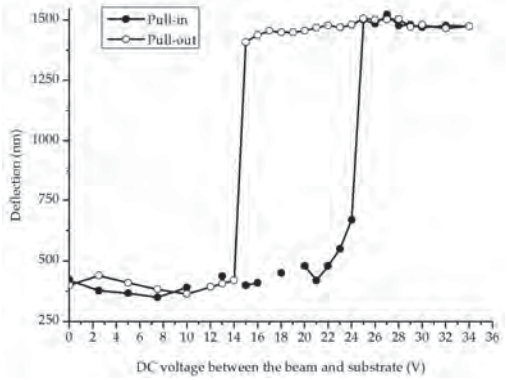

Figure 9: Displacement as a function of applied voltage for the mechanical beam. Note the pull-in voltage around 24 V.

The complete assembled device was characterized by capacitance-voltage (CV) measurements by applying bias voltage between the suspended plate and the electrodes beside the waveguide, which confirms the movement of the mechanical beam towards the waveguide, see Figure 10. The voltage range at first was kept lower than the pull-in voltage and then gradually increased until pull-in occurred. The figure shows that once pull-in has occurred the negative pull-in voltage is smaller than the positive voltage, probably due to charging of the beam. The pull-in voltage can be increased by applying another bias voltage to the highly conductive substrate to which the beam is anchored, as shown in Figure 10 for a voltage of 60V, confirming that bi-directional actuation is possible with this device.

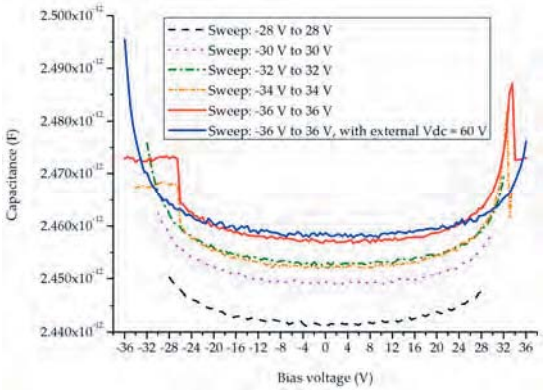

Figure 10: CV measurement for a complete assembled device. Voltage is applied between the beam and the electrodes beside the waveguide.

Optical measurements were carried out by actuating the mechanical beam using the same impedance/ gain-phase analyzer used for the CV measurements, and simultaneously monitoring the optical power with a power meter. This allowed the possibility to observe both the capacitance and the optical power output. The CV measurement confirmed the movement and pull-in of the mechanical beam towards the waveguide. However, unfortunately this did not result in a measureable change in the optical power output. With this initial optical measurement, it can be inferred that the gold coated mechanical beam is not efficient in introducing absorption loss in the optical waveguide.

CONCLUSIONS

The design and realization of a hybrid integrated mechano-optical modulator has been presented. The independent fabrication schemes of mechanical and optical chips give complete freedom for optimization and improvement. A novel self-aligned assembly technique to integrate the mechanical chip with the optical chip was also successfully realized. The bi-directional behavior of the mechanical structure has been experimentally demonstrated through CV measurements. From the initial results of optical measurements and also from simulation results, it is inferred that gold is not an optimal choice to introduce absorption loss in the optical waveguide.

ACKNOWLEDGEMENTS

The authors gratefully acknowledge the support by the Netherlands Ministry of Economic Affairs and the Netherlands Ministry of Education, Culture and Science through the Smart Mix – Memphis program.

REFERENCES

[1] W. Lukosz, "Integrated optical nano-mechanical devices as modulators, switches, tunable frequency filters and as acoustical sensors", *Proc. of the Society of photo-optical instruments*, Vol.1793, 1992.

[2] P. Pliska and W. Lukosz, "Integrated-optical acoustical sensors", *Sensors and Actuators A*, 1994.

[3] G. J. Veldhuis et al., "Electrostatically actuated mechano-optical waveguide ON/OFF switch showing high extinction at a low actuation voltage", *IEEE Journal of selected topics in Quantum Electronics*, Vol 5, No. 1, Jan/Feb 1999.

[4] G. N. Nielson et al., "Integrated wavelength selective optical MEMS switching using ring resonator filters", *IEEE Photonics Tech. letters*, vol 17, No.6, 2005.

[5] S. M. C. Abdulla et al., "Tuning a race track ring resonator by an integrated dielectric MEMS cantilever", *Optics Express*, vol 19, No.17, 2011.

[6] R. G. Heideman et al., "Low loss high contrast optical waveguides based on CMOS compatible LPCVD processing: technology and experimental results", *Proceedings symposium IEEE/LEOX Benelux chapter*, 2005.

[7] R. G. Heideman and J. A. Walker, "Surface waveguide technology for telecom and biochemical sensing", *Proc. Of SPIE*, vol. 6125, 2006.

[8] Field Designer-mode solver tool from PhoeniX BV: *http://www.phoenixbv.com*

CONTACT

M.B. Syed Nawazuddin, m.b.syednawazuddin@utwente.nl